STM JOURNALS

Journal of
Automobile Engineering and Applications

ISSN: 2455-3360
Volume 13, Issue 2, 2026
May–August
DOI Journal: 10.37591/JoAEA

https://journals.stmjournals.com/joaea

Research JoAEA

An Experimental Analysis on Enhancement of Electric Vehicle Safety using ADAS Technology and Forward Collision Avoidance with an Automatic Braking System

Bibhuti Bhusan Nayak[1]*, Md Sahariar Hossain[2], Tejash Gupta[3]

Abstract

The rapid expansion of the automobile sector in developing nations has intensified road safety concerns, particularly in congested urban environments where human error accounts for approximately 90% of all accidents. This paper presents and experimentally validates an integrated Advanced Driver Assistance System (ADAS) for electric vehicles comprising three complementary safety modules: a Forward Collision Avoidance System (FCAS) employing an HC-SR04 ultrasonic sensor interfaced with an Arduino Uno R3 to detect frontal obstacles within 50 cm and trigger automatic braking via an L298N motor driver; a Blind Spot Detection (BSD) system using three directional ultrasonic sensors with colour-coded LED alerts for lateral and rear blind zones; and a Driver Drowsiness Detection (DDD) system implemented on a Raspberry Pi 4 Model B using real-time computer vision, monitoring the Eye Aspect Ratio (EAR), Mouth Opening Ratio (MOR), and Nose Length Ratio (NLR) via the Dlib 68-point facial landmark model. Experimental results confirm reliable real-time operation of each module. The FCAS successfully engaged braking upon obstacle detection; the BSD system accurately identified directional blind-spot intrusions; and the DDD algorithm correctly classified four driver states: Active, Drowsy, Sleeping, and Head Bending with consistent accuracy across all test subjects. The proposed system is cost-effective (approximately USD 25 for hardware), modular, and scalable, providing a practical safety upgrade for commuter-segment vehicles currently underserved by commercial ADAS solutions.

Keywords: Electric vehicle safety; ADAS technology; automatic braking system; blind spot detection; driver drowsiness detection; ultrasonic sensor; eye aspect ratio; facial landmark detection

***Author for Correspondence**
Bibhuti Bhusan Nayak
E-mail: bibhuti@nitsikkim.ac.in

[1]Assistant Professor, Department of Mechanical Engineering, National Institute of Technology, Sikkim, Ravangla, South Sikkim, India
[2]Student, Department of Mechanical Engineering National Institute of Technology, Sikkim, Ravangla, South Sikkim, India
[3]Student, Department of Mechanical Engineering National Institute of Technology, Sikkim, Ravangla, South Sikkim, India

Received Date: July 17, 2026
Accepted Date: July 24, 2026
Published Date: August 18, 2026

Citation: Bibhuti Bhusan Nayak, Md Sahariar Hossain, Tejash Gupta. An Experimental Analysis on Enhancement of Electric Vehicle Safety using ADAS Technology and Forward Collision Avoidance with an Automatic Braking System. Journal of Automobile Engineering and Applications 2026; 13(2): 20–30p.

INTRODUCTION

The global proliferation of motor vehicles has led to a corresponding increase in road traffic accidents. In developing nations, insufficient infrastructure and high traffic density have made road safety a critical concern. Statistical evidence consistently indicates that approximately 90% of road accidents are attributable to human error, while road conditions (5%) and vehicle mechanical faults (5%) account for the remainder of the accidents [1]. This distribution underscores the substantial potential of driver assistance technologies to reduce accident rates.

The Automatic Emergency Braking (AEB) system, first introduced in 2009 for heavy motor vehicles and subsequently adapted for light vehicles, represents one of the most impactful ADAS interventions to date. By autonomously monitoring the forward path of the vehicle and applying a braking force when an imminent collision is detected, the AEB directly compensates for delayed human reactions. Modern AEB implementations combine radar and camera technologies to identify hazardous objects and intervene before the driver responds [2, 3].

Despite these advances in premium vehicle segments, commuter-segment vehicles continue to offer only minimal safety features, largely limited to airbags and basic engine fault diagnostics. To address this gap, the present study develops and experimentally validates a multi-module safety system integrating a Forward Collision Avoidance System (FCAS) using automatic braking, a Blind Spot Detection system with directional LED alerts, and a Driver Drowsiness Detection (DDD) system based on real-time facial landmark analysis. Together, these modules provide comprehensive, low-cost driver assistance tailored to modern electric vehicles in the commuter segment (Figure 1).

LITERATURE REVIEW

Several studies have investigated ultrasonic sensor-based obstacle detection for automotive safety. Sharma et al. [4] presented a detailed fabrication-level analysis of automatic braking systems, confirming the mechanical feasibility of such implementations in real vehicles. Ram and Kumar [5] demonstrated a basic ultrasonic braking prototype that achieved consistent distance measurements using an Arduino platform, establishing a proof-of-concept for a low-cost AEB.

In the domain of driver drowsiness detection, Sahayadhas et al. [6] provided a comprehensive review of sensor-based fatigue monitoring methods and identified camera-based facial analysis as the most practical non-intrusive approach for production vehicles. Danisman et al. [7] specifically validated eye-blink pattern analysis using camera systems for binary drowsiness classification. Liu et al. [8] proposed eyelid movement metrics consistent with the Eye Aspect Ratio computation employed in this study.

RESEARCH OBJECTIVE

The existing literature predominantly addresses individual safety subsystems in isolation. The primary contribution of this study is the integration of three complementary modules, FCAS, BSD, and DDD, within a single cost-effective hardware platform. This provides a holistic safety solution specifically aimed at the underserved commuter vehicle segment, where commercial ADAS remain economically inaccessible [9].

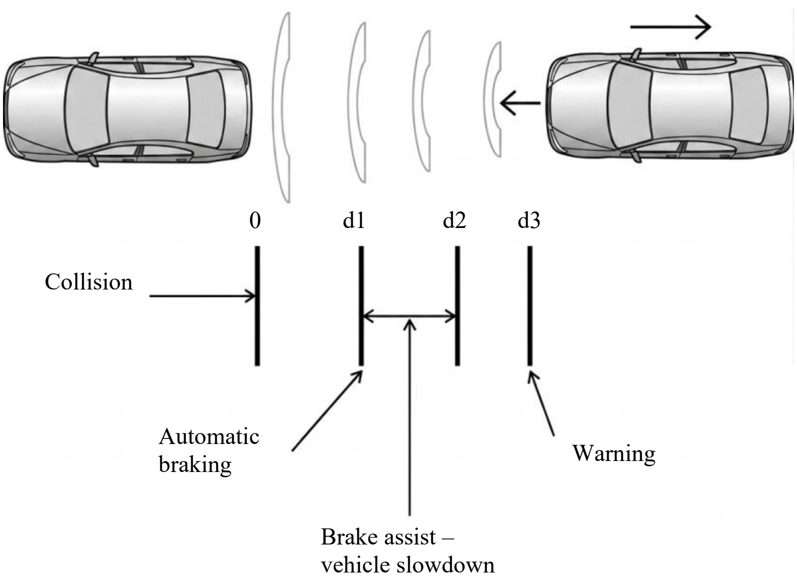

Figure 1. Schematic overview of an automatic braking system.

SYSTEM DESIGN AND HARDWARE

The proposed system is built around two primary processing units: an Arduino Uno R3, which handles sensor interfacing and motor control for the FCAS and BSD modules, and a Raspberry Pi 4 Model B (4 GB) (Figure 2) dedicated to the vision-based DDD module. The complete hardware inventory is presented in Table 1.

FORWARD COLLISION AVOIDANCE SYSTEM

Working Principle

The Forward Collision Avoidance System employs an HC-SR04 ultrasonic sensor mounted at the front of the vehicle. The sensor emits 40 kHz ultrasonic pulses via its transmitter; upon striking an obstacle, the pulse is reflected back and detected by the receiver. The Arduino Uno R3 measured the round-trip travel time and computed the obstacle distance using the speed of sound formula:

$$\text{Distance (cm)} = [\text{Time } (\mu s) \times 0.0343] \div 2$$

Table 1. System Hardware Components

Module	Component	Function
FCAS	HC-SR04 ultrasonic sensor (front)	Frontal obstacle distance measurement
FCAS	Arduino Uno R3	Sensor data processing and motor control
FCAS	L298N motor driver	DC motor braking actuation
FCAS	14.4V Li-ion battery + SPST switch	Power supply with manual isolation
BSD	HC-SR04 × 3 (left, right, rear)	Lateral and rear blind-spot detection
BSD	LEDs: white, green, blue	Directional obstacle indication
BSD	Piezo buzzer	Audible proximity warning
DDD	Raspberry Pi 4 model B (4 GB)	Computer vision pipeline host
DDD	Logitech C270 USB camera	Real-time driver face capture
DDD	Piezo buzzer (GPIO18)	Drowsiness alert output

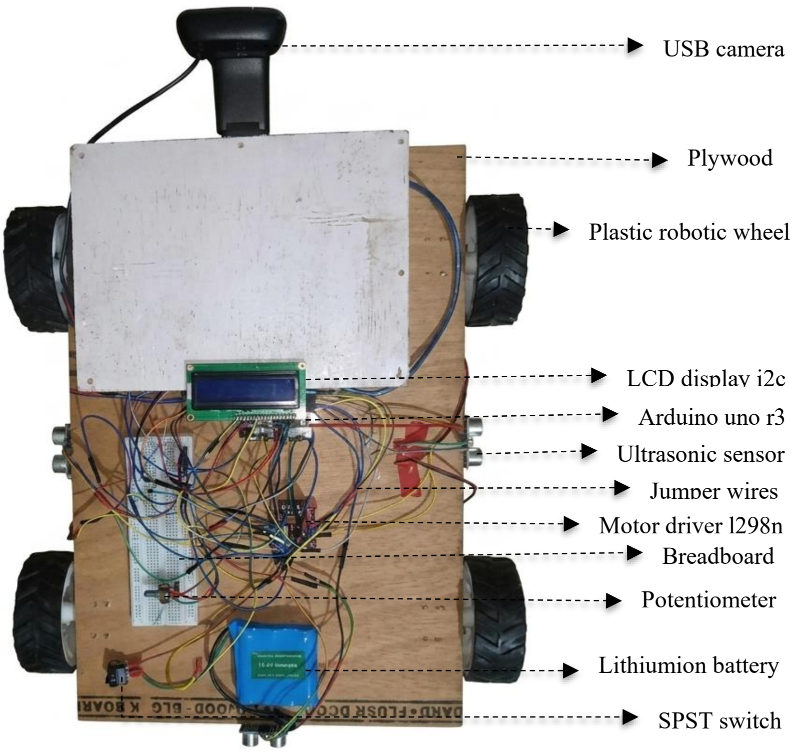

Figure 2. Experimental set-up.

When the computed distance fell at or below the safety threshold of 50 cm, the Arduino signaled the L298N motor driver to apply braking, bringing the vehicle to a controlled stop. The 50 cm threshold was empirically selected to provide a sufficient reaction margin under typical urban and low-speed driving conditions [10].

Hardware Connections

Table 2 details the pin mapping between the Arduino Uno R3 and the four ultrasonic sensors. Table 3 shows the L298N motor driver connections for controlling the four DC geared motors arranged in left and right pairs [11].

BLIND SPOT DETECTION SYSTEM

System Overview

The Blind Spot Detection system monitors three critical zones–left, right, and rear–that are not directly visible to the driver through mirrors. The system uses three HC-SR04 sensors, each paired with a dedicated color-coded LED and a shared audible piezo buzzer, as shown in Table 4. When an obstacle is detected within the 50 cm warning zone in any direction, the corresponding LED is activated, and the buzzer sounds [12].

Detection Logic

Each HC-SR04 sensor continuously scanned its assigned blind spot zone. The measured distance was compared with the 50 cm threshold.

- If distance ≤ 50 cm, the directional LED activates and the buzzer sounds obstacle present in the blind spot.
- If distance > 50 cm: LED off, buzzer silent zone clear.

To prevent acoustic cross-talk between simultaneously active sensors, sequential triggering was employed with 50–100 ms inter-sensor delays. Non-blocking timing was implemented using Arduino's millis function to ensure the continuous operation of all channels without program stalls (Table 5).

Arduino Uno, Sensor, LED and Buzzer Wiring

Incorporate this content: Components used for Blind spot detection:

- Arduino Uno R3: Acts as the main microcontroller to process sensor data and control output devices.
- Ultrasonic Sensor (HC-SR04): Measures the distance to the front obstacle using echo time.
- Breadboard and Jumper Wires: For circuit connections.
- Power Supply: Typically a 9V battery or USB power.
- Piezo Buzzer Wiring: GPIO pin is used to control the buzzer via Python.

Table 2. Arduino Uno R3 to ultrasonic sensor pin mapping.

Arduino pin	Connected component
D2 (Trig) / D3 (Echo)	Front ultrasonic sensor trigger / echo
D4 (Trig) / D5 (Echo)	Left ultrasonic sensor trigger / echo
D6 (Trig) / D7 (Echo)	Right ultrasonic sensor trigger / echo
D8 (Trig) / D9 (Echo)	Rear ultrasonic sensor trigger / echo
D10 / D11 / D12	White LED (left) / green LED (right) / blue LED (rear)
5V / GND	Breadboard positive and negative power rails

Table 3. L298N Motor driver output connections.

L298N output	Motor connection
OUT1 / OUT2	Left motor pair positive (+) / negative (−)
OUT3 / OUT4	Right motor pair positive (+) / negative (−)

Table 4. LED Colour to sensor direction mapping.

Sensor direction	LED colour	Arduino pin	Risk scenario
Left	White	D10	Lane change; left turns; overtaking from left
Right	Green	D11	Lane switching to right; highway merging
Rear	Blue	D12	Reversing; parking; small obstacles behind vehicle

Table 5. Raspberry Pi 4 GPIO piezo buzzer connection.

Buzzer terminal raspberry Pi GPIO
Positive (+) RED WIre GPIO18 (physical pin 12)
Negative (−) black wire GND (physical pin 6)

Table 6. Dlib 68-point facial landmark distribution by region.

Facial region	Landmark point range
Jawline	0 – 16
Right eyebrow	17 – 21
Left eyebrow	22 – 26
Nose bridge	27 – 30
Lower nose	31 – 35
Right eye	36 – 41
Left eye	42 – 47
Outer lips	48 – 59
Inner lips	60 – 67

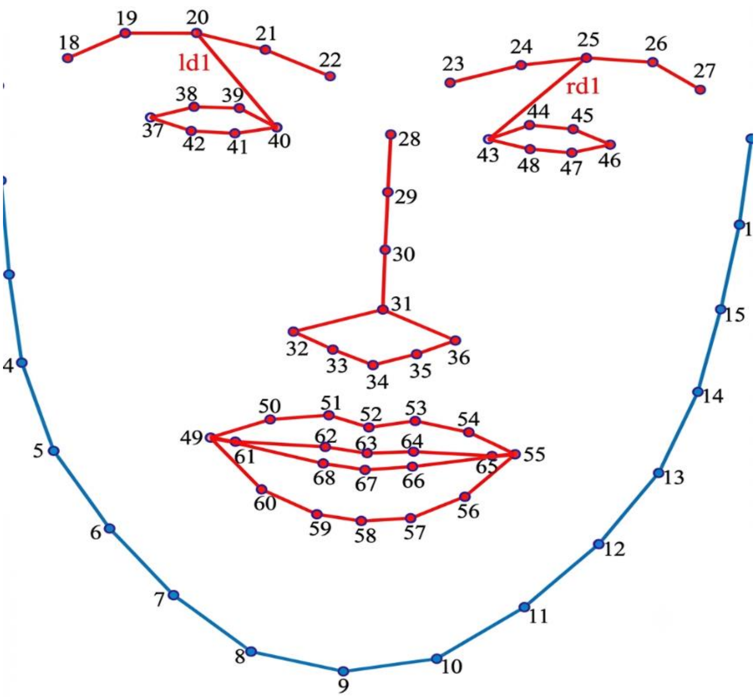

Figure 3. Dlib 68-point facial landmark annotation on a human face.

DRIVER DROWSINESS DETECTION SYSTEM

Motivation

According to the National Highway Traffic Safety Administration (NHTSA) and the World Health Organization (WHO), drowsy driving is a major contributor to road fatalities, with impairment levels comparable to alcohol intoxication. Fatigue accumulates, particularly during long-distance highway driving, night shifts, and monotonous road conditions. Unlike alcohol impairment, drowsiness produces no externally visible behavioral cues and goes undetected by law enforcement, making automated in-vehicle detection systems indispensable.

Dlib 68-Point Facial Landmark Model

The drowsiness detection pipeline was built using Dlib's pre-trained 68-point facial landmark model. The model uses a Histogram of Oriented Gradients (HOG) + SVM-based face detector to locate the face region, followed by supervised landmark prediction using the shape_predictor_68_face_landmarks.dat model (Figure 3). The 68 landmarks were distributed across the facial regions, as described in Table 6.

Eye Aspect Ratio (EAR)

The Eye Aspect Ratio quantifies eye openness as the ratio of vertical eye height to horizontal eye width, computed from six peri-ocular landmarks (p1–p6) as follows:

$$EAR = (||p2 - p6|| + ||p3 - p5||) / (2 \times ||p1 - p4||)$$

When the eyes were open, the vertical distances (numerator) were significant, yielding a higher EAR value. Progressive eye closure reduces the numerator to zero. An EAR below 0.20 sustained over multiple consecutive frames is interpreted as eye closure, indicative of drowsiness or microsleep. The typical EAR ranges are listed in Table 7.

Mouth Opening Ratio (MOR)

The Mouth Opening Ratio measures mouth aperture as an indicator of yawning, which is a well-established physiological correlate of fatigue. The MOR is computed using outer-lip landmarks where p48 and p54 are the horizontal corners, and p51 and p57 are the vertical lip extremities.

$$MOR = ||p51 - p57|| / ||p48 - p54||$$

A temporal threshold requiring MOR > 0.6 sustained for more than two seconds was applied to distinguish a genuine yawning event from normal speech or brief mouth opening. The typical MOR values across the mouth states are presented in Table 8.

Nose Length Ratio (NLR)

The Nose Length Ratio captures head pose variation, particularly forward head tilt (nodding), which is a characteristic postural precursor to sleep onset. The NLR is defined as the ratio of the perceived vertical nose length in the image space to a reference facial measurement, such as the interocular distance:

NLR = Vertical nose length (image) / Interocular distance

A forward head tilt compresses the apparent nose length, reducing the NLR below its neutral baseline of approximately 0.90–1.10. A 15–30 frame temporal smoothing window was applied to suppress noise-induced false positives. The expected NLR ranges are summarized in Table 9.

Table 7. Typical EAR values by eye state.

Eye state	Typical EAR value
Open (alert)	0.25 – 0.30
Drowsy / half-closed	0.20 – 0.25
Closed (blink / sleep)	< 0.20

Table 8. Mouth opening ratio (MOR) vs. mouth state.

Mouth state	Approximate MOR range
Closed	0.20 – 0.35
Talking / slightly open	0.35 – 0.60
Yawning	0.60 – 1.00+

Journal of Automobile Engineering and Applications
Volume 13, Issue 2
ISSN: 2455-3360

Table 9. Head pose vs. nose length ratio (NLR).

Head pose	Approximate NLR range
Neutral (awake)	0.90 – 1.10
Forward tilt (drowsy)	0.08 – 0.90
Backward tilt	0.08 – 0.70

Detection Pipeline

The Raspberry Pi 4 captured live video via the Logitech C270 USB camera and processed each frame through the following sequential pipeline: (1) face detection using the Dlib HOG+SVM detector; (2) 68-point facial landmark localization; (3) computation of EAR, MOR, and NLR from the relevant landmark coordinates; (4) thresholding and temporal consistency evaluation across the sliding frame window; and (5) activation of the piezo buzzer via GPIO18 upon confirmed drowsiness classification. This pipeline runs entirely on a Raspberry Pi 4 without requiring an external server or cloud connection.

RESULTS AND DISCUSSION

FCAS and BSD Validation

The Forward Collision Avoidance System successfully applied automatic braking in all test scenarios in which an obstacle was introduced within the 50 cm threshold. No false triggers were recorded during the repeated open-road test runs. The Blind Spot Detection system correctly activated the color-coded LED and buzzer alerts for all three sensor directions in every trial. Figures 4–6 confirm the LED activation states observed during the hardware testing.

Driver Drowsiness Detection Results

Four driver states were evaluated: Active, Drowsy, Sleeping, and Head Bending. Three participants were involved in each state classification session. The EAR, MOR, and NLR were plotted over 60 video frames for each condition and analyzed. Table 10 summarizes the mean metric values and alert statuses for each state.

Active State

In the active state, the EAR remained stable between 0.25 and 0.35 (mean 0.338), consistent with open and alert eyes. The MOR was consistently low at 0.016, indicating no yawning or sustained mouth opening. The NLR was steady at 0.101, reflecting an upright and neutral head posture. These three metrics together confirm an alert, attentive driver posture, and no alert was triggered (Figure 7).

Drowsy State

The drowsy state exhibited a notable EAR dip near frame 45 (approaching 0.20), indicating an incipient eye closure. The MOR showed transient spikes at frames 18 and 50 (mean 0.194), consistent with yawning events. The NLR remained stable at 0.107, indicating no significant head movement during this stage. The co-occurrence of an EAR drop and MOR spike within the same temporal window constitutes a robust composite drowsiness signal that reliably triggers an alert (Figure 8).

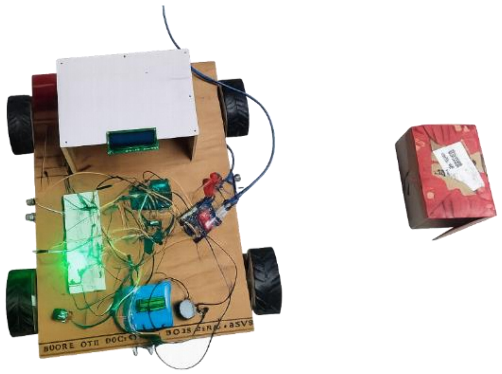

Figure 4. Right sensor detection green LED activated (obstacle within 50 cm).

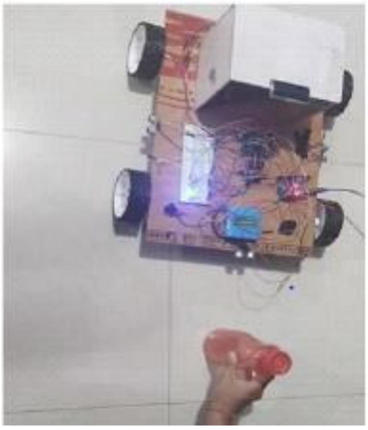

Figure 5. Rear sensor detection blue LED activated (obstacle within 50 cm).

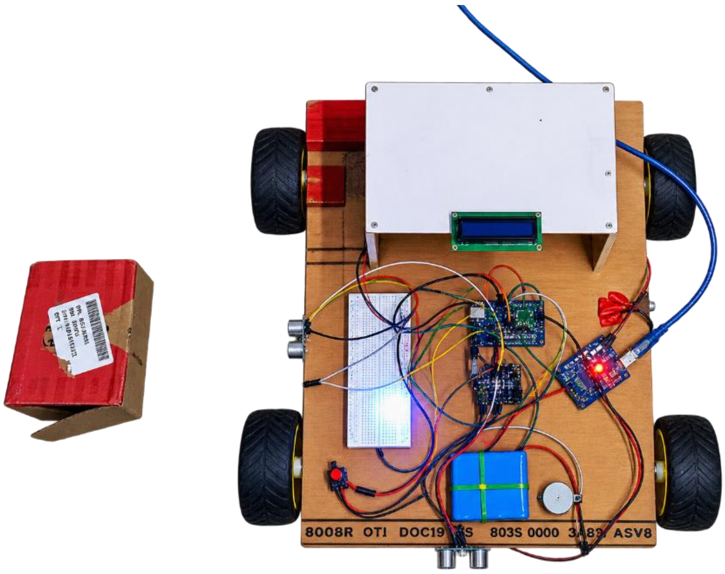

Figure 6. Left sensor detection white LED activated (obstacle within 50 cm).

Table 10. Mean facial metric values across driver states.

Driver state	Mean EAR	Mean MOR	Mean NLR	Alert triggered
Active	0.338	0.016	0.101	No
Drowsy	0.339	0.194	0.107	Yes (EAR dip + MOR spike)
Sleeping	0.140	0.016	0.101	Yes (persistent EAR < 0.20)
Head bending	0.321	0.033	0.073	Yes (NLR below baseline)

Sleeping State

In the sleeping state, the EAR was persistently low across all frames (mean 0.140), well below the 0.20 threshold, indicating sustained eye closure consistent with stage 1 sleep onset. The MOR was low (mean 0.016), suggesting that the subject had progressed beyond the active yawning phase into early sleep. A stable NLR (0.101) reflects a stationary resting posture. These combined readings are characteristic of a driver who has entered light sleep in a real-time system, and such readings would immediately trigger a sustained alert (Figure 9).

Head Bending State

The head bending condition yielded a distinctive metric signature: EAR remained within the normal awake range (mean 0.321), indicating that the eyes were still open, while NLR was significantly depressed (mean 0.073), well below the neutral 0.90–1.10 baseline. This reduction reflects a forward chin tilt, which reduces the perceived vertical nose length. The MOR was slightly elevated at 0.033 relative to the sleeping state, attributable to light mouth movement during early fatigue. The combination of a normal EAR with a low NLR provides an early fatigue indicator that precedes eye closure, enabling preemptive alerting before the driver enters a more advanced drowsiness stage (Figure 10).

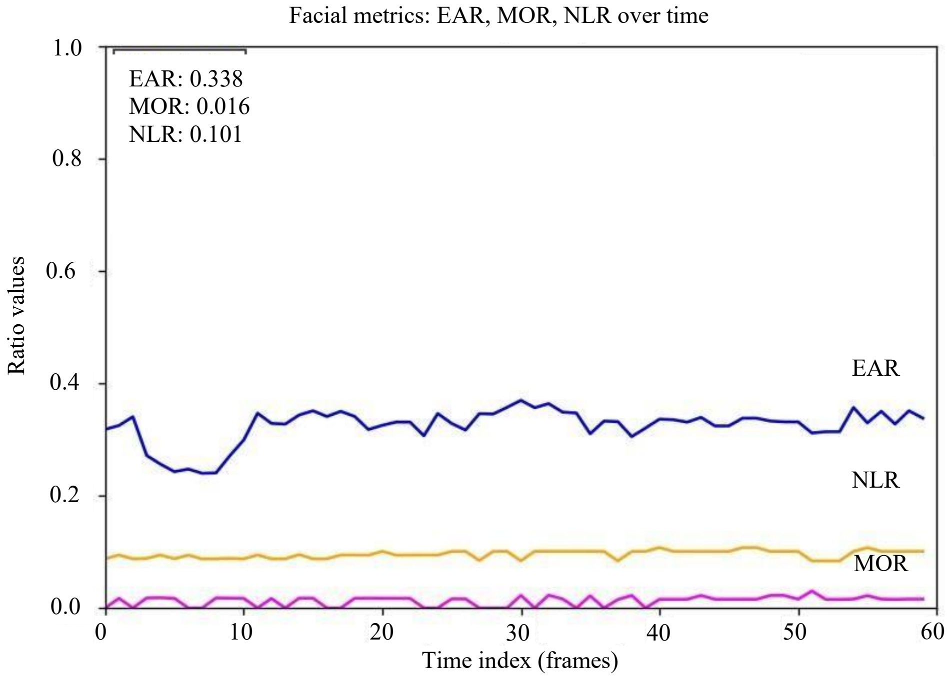

Figure 7. Facial metric graph active state (EAR: 0.338, MOR: 0.016, NLR: 0.101).

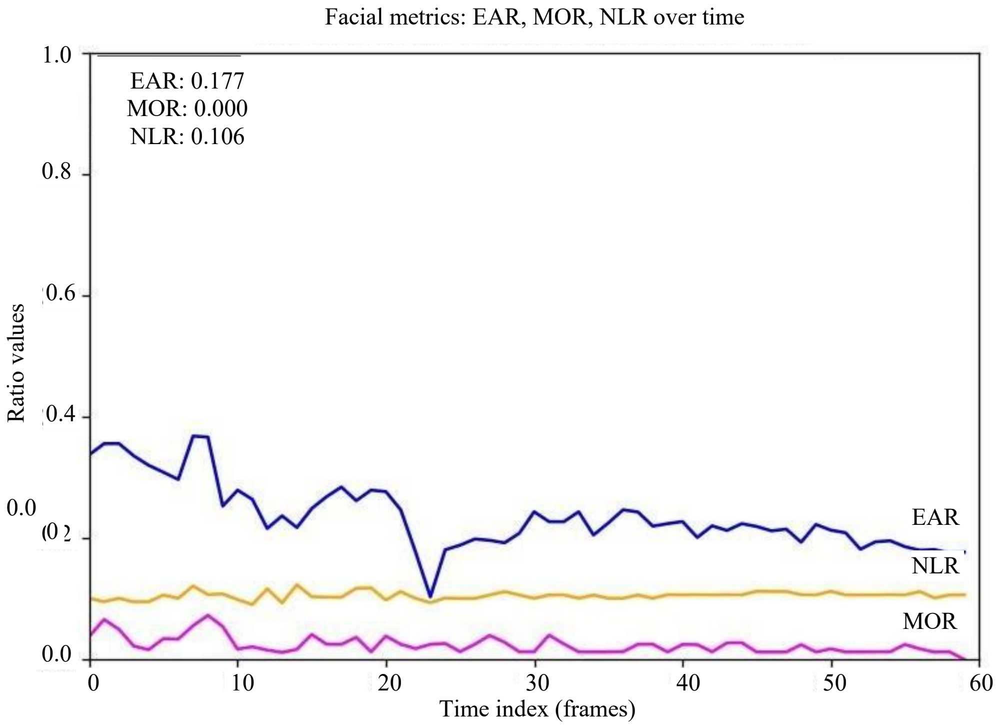

Figure 8. Facial metric graph drowsy state (EAR: 0.339, MOR: 0.194, NLR: 0.107).

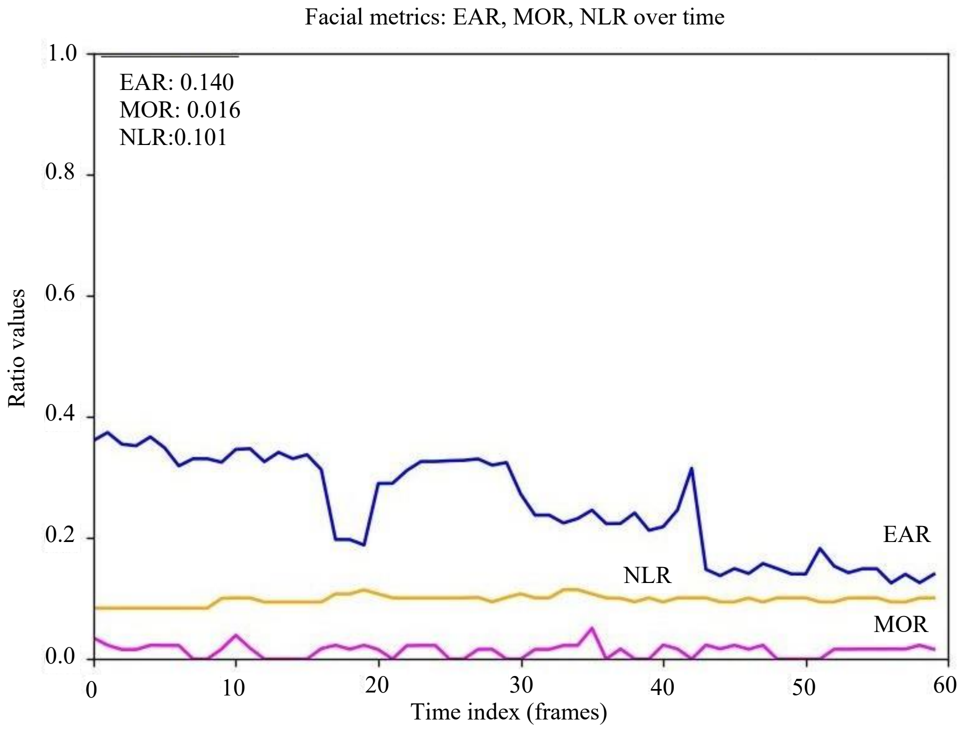

Figure 9. Facial metric graph sleeping state (EAR: 0.140, MOR: 0.016, NLR: 0.101).

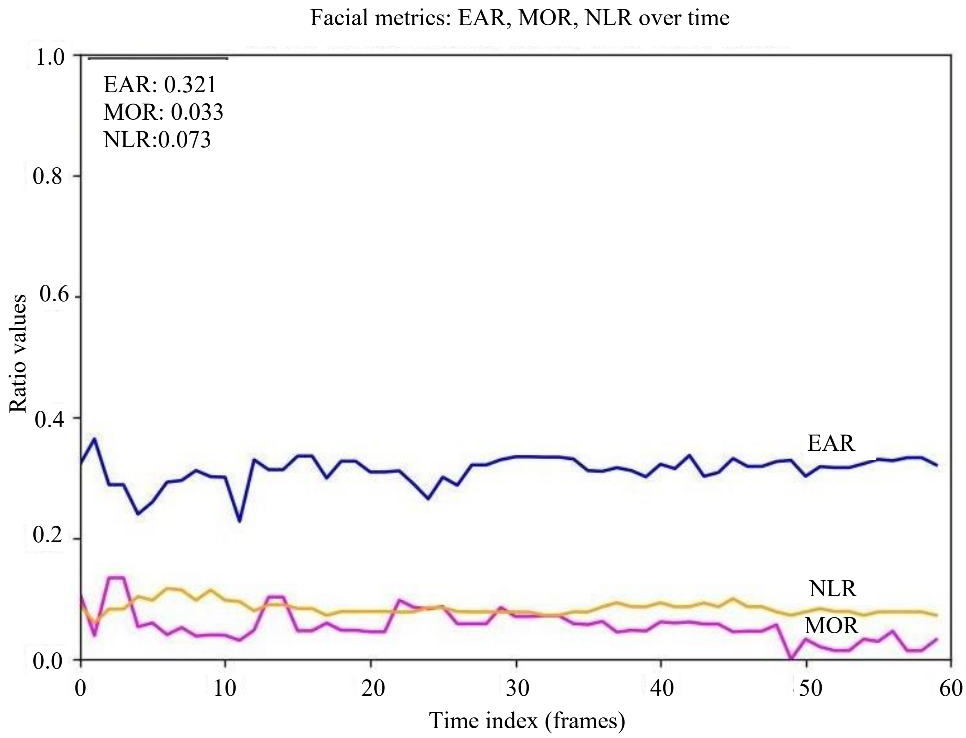

Figure 10. Facial metric graph Head Bending state (EAR: 0.321, MOR: 0.033, NLR: 0.073).

CONCLUSIONS

This study presented and experimentally validated an integrated ADAS framework comprising three complementary safety modules for electric vehicles. The Forward Collision Avoidance System reliably applied automatic braking whenever obstacles were detected within a 50 cm threshold, with no false triggers recorded. The Blind Spot Detection system accurately produced directional LED and audible alerts for all tested scenarios across the left, right, and rear sensor channels. The Driver Drowsiness Detection system successfully classified four distinct driver states: Active, Drowsy, Sleeping, and Head Bending, using a three-parameter facial metric model (EAR, MOR, and NLR). Notably, the EAR+NLR combination provided a sensitive early fatigue indicator that precedes full eye closure, enabling pre-emptive alerting at the head-bending stage before dangerous drowsiness sets in.

The system is constructable at approximately USD 25 for the sensor hardware modules, is fully modular and independently testable per subsystem, and offers a practical safety upgrade for commuter-segment vehicles that are currently underserved by commercial ADAS products. The proposed architecture can serve as a foundational platform for future sophisticated implementations.

REFERENCES

1. Schram, R., Williams, A., van Ratingen, M., 2013. Implementation of Autonomous Emergency Braking (AEB), the next step in Euro NCAP's safety assessment. Proc. 23rd International Technical Conference on the Enhanced Safety of Vehicles (ESV), Seoul, Korea.
2. Xia, L., Chung, T. D., Kassim, K. A. B. A., 2013. A review of the automated emergency braking system and the trends for future vehicles. Proc. Southeast Asia Safer Mobility Symposium.
3. Sidek, S. N., & Salami, M. J. E. 2000. Design of an intelligent braking system. Proc. TENCON 2000: Intelligent Systems and Technologies for the New Millennium, IEEE. 2, 580–585.
4. Ram, J., & Kumar, B., 2017. Automatic braking system using an ultrasonic sensor. International Journal of Innovative Science and Research Technology. 2(4), 2456–2165.
5. Sharma, Y., Singh, S. S., Nawaz, M., Kaushik, V., Sharma, S., Sindhwani, R., Singh, P. L.,2021. Design, analysis, and fabrication of automatic braking system. Advances in Engineering Design. Springer, Singapore. 541–550.
6. Sahayadhas, A., Sundaraj, K., Murugappan, M., 2012. Detecting driver drowsiness based on sensors: A review. Sensors. 12(12), 16937–16953.
7. Danisman, T., Bilasco, I. M., Djeraba, C., Ihaddadene, N., 2010. Drowsy driver detection system using eye blink patterns. Proc. International Conference on Machine and Web Intelligence (ICMWI). IEEE. 230–233.
8. Liu, D., Sun, P., Xiao, Y., Yin, Y., 2010. Drowsiness detection based on eyelid movement. Proc. 2nd International Workshop on Education Technology and Computer Science (ETCS). IEEE. 49–52.
9. Deotale, M. S., Shivankar, H., More, R., 2016. Review on intelligent braking system. International Journal on Recent and Innovation Trends in Computing and Communication. Retrieved from http://www.ijritcc.org
10. Dong, Y., Hu, Z., Uchimura, K., Murayama, N. 2011. Driver inattention monitoring system for intelligent vehicles: A review. IEEE Transactions on Intelligent Transportation Systems. 12(2), 596–614.
11. Bila, C., Sivrikaya, F., Khan, M. A., Albayrak, S., 2017. Vehicles of the future: A survey of research on safety issues. IEEE Transactions on Intelligent Transportation Systems, 18(5), 1046–1065.
12. Qing, W., BingXi, S., Bin, X., Junjie, Z., 2010. A PERCLOS-based driver fatigue recognition application for smart vehicle space. Proc. 3rd International Symposium on Information Processing (ISIP). IEEE. 437–441.

